

## Conclusions

Unsteady laminar boundary layers exhibit quite different behavior, depending on whether the freestream perturbations consist of a standing wave or traveling waves. For standing-wave freestream conditions, there is a phase lead of the velocity in the inner layer, reaching a maximum value of 45 deg at high values of reduced frequency. For traveling-wave freestream conditions, two parameters, the reduced frequency  $\bar{\omega}$  and the traveling-wave convection velocity ratio  $Q/U_0$ , are required to fully describe the flow. With a freestream subject to traveling waves and with  $Q/U_0$  less than about 2.0, the boundary-layer velocity exhibits a phase lag with respect to the freestream that increases with decreasing values of  $Q/U_0$ . The calculation method can be extended to turbulent boundary layers subject to traveling waves by incorporating the eddy viscosity model of Cebeci and Carr.

## Acknowledgments

The author is grateful to the Director, staff, and students of the Whittle Laboratory, Cambridge University Engineering Department, for many helpful discussions during the preparation of this Note.

## References

- <sup>1</sup>Evans, R. L., "Boundary Layer Development on an Axial-Flow Compressor Stator Blade," *ASME Journal of Engineering for Power*, Vol. 100, April 1978, pp. 287-293.
- <sup>2</sup>Cebeci, T. and Carr, L. W., "A Computer Program for Calculating Laminar and Turbulent Boundary Layers for Two-Dimensional Time-Dependent Flows," NASA TM-78470, March 1978.
- <sup>3</sup>Lighthill, M. J., "The Response of Laminar Skin Friction and Heat Transfer to Fluctuations in the Stream Velocity," *Proceedings of the Royal Society of London*, Vol. 224A, 1954, pp. 1-23.
- <sup>4</sup>Patel, M. H., "On Laminar Boundary Layers in Oscillatory Flow," *Proceedings of the Royal Society of London*, Vol. 347A, 1975, pp. 99-123.
- <sup>5</sup>Evans, R. L., "Unsteady Laminar Boundary Layers Subject to Standing Wave or Traveling Wave Freestream Fluctuations," Cambridge Univ. Engineering Dept., Cambridge, England, Rept. CUED/A-Turbo/TR 124, 1988.

# Shock-Wave/Boundary-Layer Interaction at a Swept Compression Corner

Oktaý Özcan\* and M. Orhan Kaya†  
Istanbul Technical University, Istanbul, Turkey

## Introduction

IN supersonic flow over a compression corner mounted on a flat plate, a shock wave is formed ahead of the compression corner. The adverse pressure gradient caused by the shock wave propagates upstream through the subsonic portion of the boundary layer developing on the flat plate. The interaction of the shock wave with the boundary layer can lead to flow separation if the shock wave is sufficiently strong. In the case

of swept compression corners, the resulting interaction is too complex for significant analytical treatment, and, therefore, experimental data are necessary to understand the flow physics. Such data are reported by Refs. 1, 2, and 3. A numerical solution of the separated flow problem is given by Horstman.<sup>4</sup>

A sketch of the swept compression corner geometry is given in Fig. 1. The quantities  $\alpha$  and  $\lambda$  are the compression angle and sweep angle, respectively. The separation angle  $\beta$  is defined as the angle between the separation line and the spanwise direction  $z$ . Settles and Teng<sup>3</sup> report the existence of two distinct flow regimes, which are referred to as cylindrical and conical. The separation line and the corner line make an angle with each other in the conical flow regime ( $\beta \neq \lambda$ ), whereas the two lines are parallel in the cylindrical flow regime ( $\beta = \lambda$ ). Settles and Teng<sup>3</sup> propose the "Shock Detachment Hypothesis," which states that the transition from the cylindrical flow to the conical flow regime is due to the detachment of the shock wave that is otherwise attached to the corner for small  $\alpha$  and  $\lambda$ .

The present note reports results of an experimental study carried out at Mach numbers between 1.8 and 2.2. Data were obtained by oil flow visualization. A third flow regime was observed in addition to the cylindrical and conical flow regimes. The new regime reveals itself when the Mach number to the corner line ( $M_n$ ) is around one. Results of the study lend support to the "Shock Detachment Hypothesis."

## Experiments

The experiments were conducted in the 60 × 30 mm Trisonic Wind Tunnel at the Istanbul Technical University. This facility is a continuous tunnel operating at atmospheric stagnation conditions. The freestream Mach number was varied by changing the shape of the Laval nozzle upstream of the test section. The freestream Reynolds number per unit length was  $12.7 \times 10^6$  (1/m) at Mach 2.2.

The model geometry is defined by the parameters  $\alpha$ ,  $\lambda$ ,  $t$ , and  $L$ , which are shown in Fig. 1. The models were made of plexiglas ( $t = 4$  mm,  $L = 50$  mm) and were mounted on the side wall of the tunnel. Approximately 30 models with various values of  $\alpha$  and  $\lambda$  were used in the experiments. The thickness of the fully developed turbulent boundary layer on the tunnel side wall was approximately 8 mm at the test section. The fact that model thickness  $t$  was smaller than boundary layer thickness  $\delta$  was an interesting feature of the present study. In all previous studies of the flow  $t$  was larger than  $\delta$  and the interaction was "dimensionless," that is, the model thickness did not impose a length dimension on the interaction characteristics. The interaction of the present study was probably dimensional. However, this was not verified by varying the model thickness systematically.

Oil flow visualization was made to observe the topology of the skin-friction line pattern on the flat plate. A mixture of titanium dioxide, oleic acid, and engine oil was used in oil flow visualization. The separation angle ( $\beta$ ) was measured from the oil flow photographs taken during a tunnel run with an accuracy of  $\pm$  one degree.

## Discussion of Results

Oil flow visualization revealed three characteristic flow regimes. Figure 2 gives a schematic description of the flow

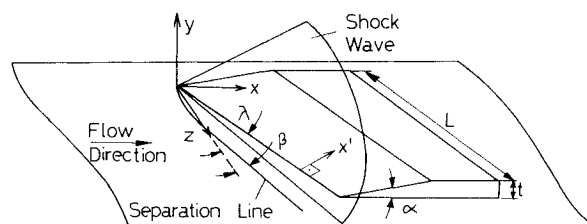


Fig. 1 A schematic view of the swept compression corner geometry.

Received Jan. 5, 1989; revision received March 20, 1989. Copyright © 1989 by American Institute of Aeronautics and Astronautics, Inc. All rights reserved.

\*Associate Professor, Faculty of Aeronautics and Astronautics; currently Senior NRC Associate at NASA-ARC, CA. Member AIAA.

†Graduate Student, Faculty of Aeronautics and Astronautics.

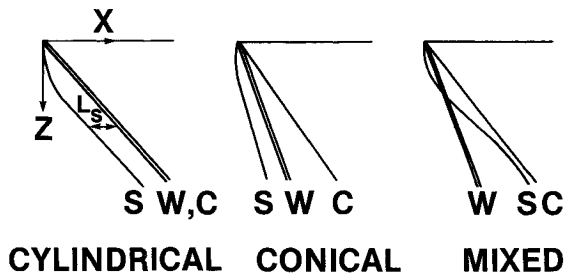


Fig. 2 A schematic description of the characteristic flow regimes.

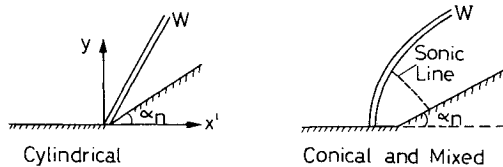


Fig. 3 Shock wave structure in the  $(x'-y)$  plane normal to the corner.

regimes, named as cylindrical, conical, and mixed. The separation line, the shock wave, and the corner line are denoted by the letters S, W, and C, respectively.  $L_s$  is the separation distance measured between the separation line and the corner line in streamwise direction  $x$ . In the cylindrical regime,  $L_s$  increases with increasing  $z$  and reaches an asymptotic value that remains constant for larger  $z$  values. In the conical regime,  $L_s$  increases monotonically with  $z$  and is a linear function of the spanwise distance for large  $z$  values. Due to the existence of inception lengths, the cylindrical and conical flow regime were originally called "quasi-cylindrical" and "quasi-conical" in Ref. 3. The third flow regime which is called the "mixed flow," can be perceived as a mixture of the conical and cylindrical regimes. In the mixed flow  $L_s$  first increases and then decreases with increasing  $z$  before reaching a constant value.

Figures 2 and 3 depict the hypothesized cross sections of the three-dimensional shock wave in the flat plate plane ( $x-z$ ) and in the  $(x'-y)$  plane where the  $x'$  direction is perpendicular to the corner line. In Fig. 3,  $\alpha_n$  is the compression angle normal to the corner. The value of  $\alpha_n$  is equal to  $\arctan(\tan\alpha/\cos\lambda)$ . The mixed flow is observed to occur for  $M_n$  values around one ( $M_n = M \cos\lambda$ ). It can be hypothesized that in the conical and mixed flows,  $M_n$  values are not large enough to deflect the flow by angle  $\alpha_n$ . Thus, there exists a detached shock wave and a subsonic flow region ahead of the corner line. It can be further hypothesized that in the mixed flow, the shock wave is not strong enough to cause boundary-layer separation at large spanwise distances. Consequently, as shown in Fig. 2, the separation line (oil accumulation line) crosses the inviscid shock projection and runs parallel to the corner line for large  $z$  values. In the case of glancing shock-wave boundary-layer interactions, Korkegi<sup>5</sup> report that incipient boundary-layer separation occurs when the Mach number normal to the skewed shock-wave is 1.2. A check on the applicability of Korkegi's criteria to the flow of the present study could not be made because the shock angle in the  $x-z$  plane was not known. The fact that the model thickness was smaller than the boundary-layer thickness may have played a role in bringing the effective Mach number down and causing the mixed flow.

The characteristic flow regimes observed for various models at Mach 2.2 are shown on a  $(\alpha, \lambda)$  diagram in Fig. 4a. The boundary between the cylindrical and conical regimes as predicted by the shock detachment hypothesis is also shown. Figure 4b shows the characteristic flow regimes at various Mach numbers on a  $(\alpha, \lambda)$  diagram. The numerals under the symbols indicate the Mach numbers. The shock detachment boundaries at Mach 2.0 and 2.2 are shown by two separate

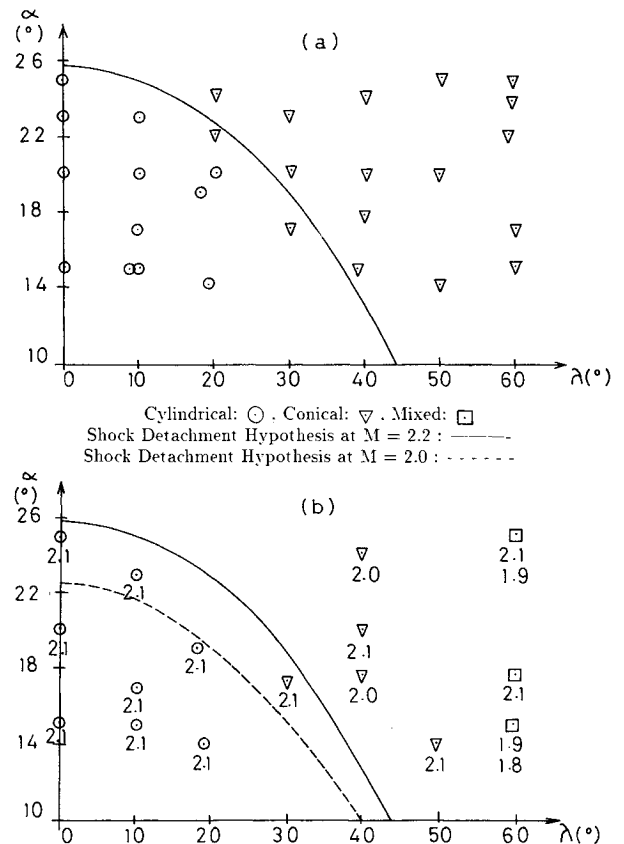


Fig. 4 Characteristic flow regimes on  $(\alpha, \lambda)$  diagrams.

curves. Observation of conical flows for  $(\alpha, \delta)$  pairs below the shock detachment curve is also reported by Settles and Teng.<sup>3</sup> This is probably due to a decrease of the effective Mach number within the boundary layer.

Figure 4 shows that the mixed flow regime is observed at Mach numbers smaller than 2.2 when the Mach number normal to the corner line ( $M_n$ ) is around one. Settles and Teng<sup>3</sup> did not report the mixed flow probably because of the fact that the minimum value of  $M_n$  in their experiments was 1.5. The shock detachment hypothesis was proposed on the basis of experimental data obtained at a single Mach number of 2.95 (Ref. 3). The results presented in Fig. 4 lend support to the validity of this hypothesis. Low-speed data obtained in the present study showed that the cylindrical flow was the only regime existing in subsonic flow. This characteristic of the subsonic flow, which is free from shock waves, also provides an indirect support for the validity of the shock detachment hypothesis.

## Conclusions

An experimental investigation of the supersonic turbulent separated flow over a swept compression corner was made. Conclusions of the study can be listed as follows:

- 1) Three characteristic flow regimes referred to as cylindrical, conical, and mixed were identified.
- 2) The mixed flow regime was observed to occur when the Mach number normal to the corner was around one.
- 3) The high speed data obtained in the study lent direct support for the validity of the "Shock Detachment Hypothesis."
- 4) Indirect support for the validity of the "Shock Detachment Hypothesis" was provided by the low speed data, which showed that the turbulent subsonic flow was always cylindrical.

## Acknowledgment

This study was supported by the UYG-AR Applied Research Center of Istanbul Technical University.

### References

- <sup>1</sup>Bachalo, W. D. and Holt, M., "Three-Dimensional Boundary Layer Separation in Supersonic Flow," *AGARD Conference Proceedings*, No. 168, Göttingen, Federal Republic of Germany, 1975.
- <sup>2</sup>Settles, G. S. and Bogdonoff, S. M., "Scaling of Two- and Three-Dimensional Shock/Turbulent Boundary-Layer Interactions at Compression Corners," *AIAA Journal*, Vol. 20, June 1982, pp. 782-789.
- <sup>3</sup>Settles, G. S. and Teng, H. Y., "Cylindrical and Conical Flow Regimes of Three-Dimensional Shock/Boundary-Layer Interactions," *AIAA Journal*, Vol. 22, Feb. 1984, pp. 194-200.
- <sup>4</sup>Horstman, C. C., "A Computational Study of Complex Three-Dimensional Compressible Turbulent Flow Fields," *AIAA Journal*, Vol. 23, No. 10, 1985, pp. 1461-1462.
- <sup>5</sup>Korkegi, R. H., "A Simple Correlation for Incipient Turbulent Boundary-Layer Separation due to a Skewed Shock-wave," *AIAA Journal*, Vol. 11, No. 11, 1973, pp. 1578-1579.

## Critique of Turbulence Models for Shock-Induced Flow Separation

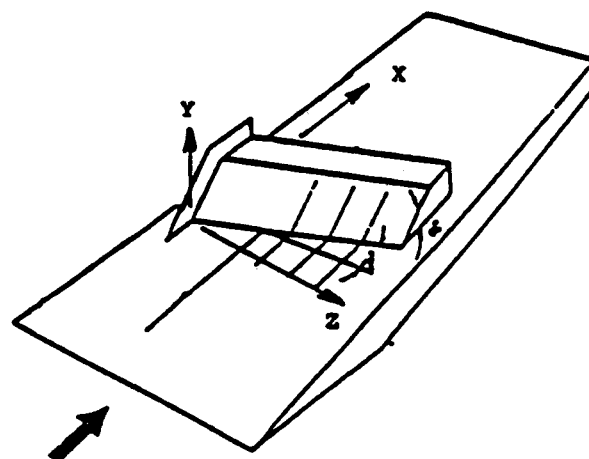
L. E. Ericsson\*

Lockheed Missiles & Space Company, Inc.,  
Sunnyvale, California

RECENT results for a 60-deg swept 24-deg ramp at  $M \approx 3$  show poor agreement between Navier-Stokes computations and experiment<sup>1</sup> (Fig. 1). Whether the flat plate leading edge was assumed to be straight or swept 60 deg had little impact on the computations (compare cases 1 and 2 with case 3). Going from the Baldwin-Lomax to the Jones-Launder turbulence model appeared to improve prediction somewhat (compare cases 3 and 4, respectively), until the streamwise grid spacing was refined (case 5), when the comparison became as bad as for cases 1-3. As it is well known that prediction of pressures is a very mild test of a computational method, the results in Fig. 1 give cause for concern. Obviously the computations, although performed by well-recognized experts in the field, do not simulate all aspects of the physical flow phenomenon involved.

The computational flow model of Ref. 1 is shown in Fig. 2a. It contains only a primary separation with associated vortex. This contrasts with the flow picture evolving from swept-fin experiments<sup>2</sup> (Fig. 2b), where both secondary and tertiary flow separations with associated vortices were identified. Supersonic experimental results for a sharp-edged delta wing also show the presence of secondary flow separation<sup>3</sup> (Fig. 3). One asks oneself if all three types of flow separation are not very similar, and that the likely reason for the poor agreement between prediction and experiment in Fig. 1 is the failure to include correctly secondary flow separation effects in the numerical simulation.

Using a skin-friction visualization technique, Szodruch and Monson<sup>4</sup> have determined the positions of separation and attachment lines on a 70-deg delta wing at  $M = 3$  (Fig. 4). Primary and secondary flow separation features are outlined in detail, with flow attachment ( $A_1$ ,  $A_2$ , and even  $A_3$ ) causing a significant increase in skin friction.



Case No.	Turb model	Leading edge	$x_u/\delta_\infty$	$M_\infty$	$\delta_\infty$ (cm)	$Re_{\delta_\infty}$	Total pressure (kPa)	Total temp. (deg K)
1	B-L	Straight	n/a	2.95	0.22	$1.4 \times 10^5$	689	266
2	B-L	Straight	n/a	2.95	0.22	$1.4 \times 10^5$	689	266
3	B-L	Swept	26.2	2.95	0.39	$2.3 \times 10^5$	689	275
4	J-L	Swept	40.4	2.95	0.39	$2.3 \times 10^5$	689	275
5	J-L	Swept	40.3	2.95	0.39	$2.3 \times 10^5$	689	275

B-L Baldwin-Lomax; J-L Jones-Launder; n/a not applicable

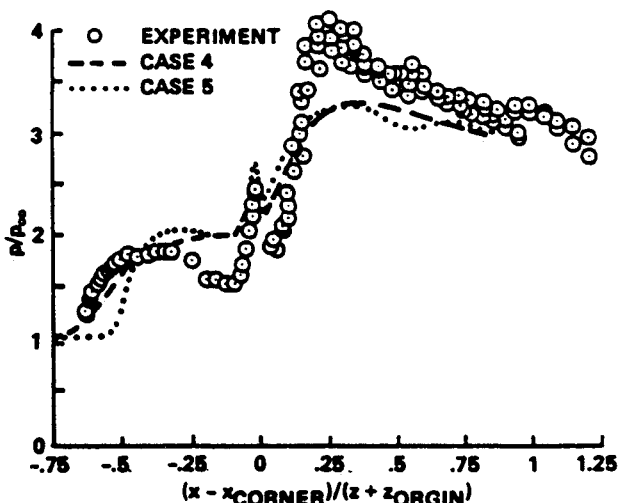
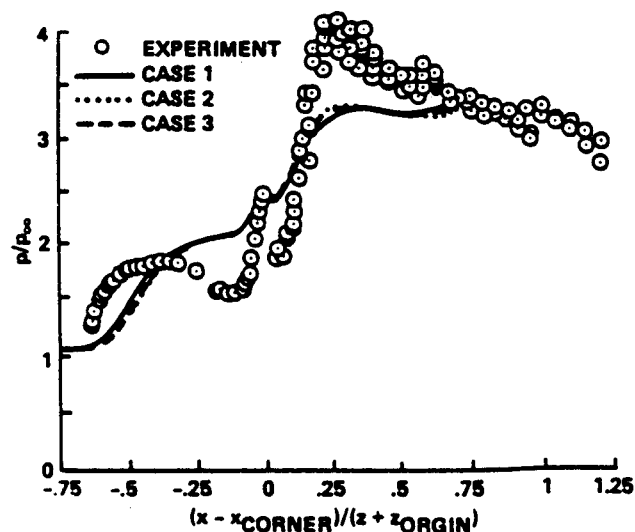


Fig. 1 Supersonic turbulent flow at Mach 3 past a 60-deg swept 23-deg compression corner.<sup>1</sup>

Presented as part of Paper 88-3525 at the 1st National Fluid Dynamics Congress, Cincinnati, OH, July 25-28, 1988; received Sept. 9, 1988; revision received Jan. 23, 1989. Copyright © by L. E. Ericsson, published by the American Institute of Aeronautics and Astronautics, Inc. with permission

\*Senior Consulting Engineer. Fellow AIAA.